

## Article

# Edge Currents Induced by AC Electric Field in Two-Dimensional Dirac Structures

Mikhail V. Durnev  and Sergey A. Tarasenko \*

Ioffe Institute, Politechnicheskaya 26, 194021 St. Petersburg, Russia

\* Correspondence: tarasenko@coherent.ioffe.ru

**Abstract:** Edges in two-dimensional structures are the source of nonlinear transport and optical phenomena which are particularly important in small-size flakes. We present a microscopic theory of the edge photogalvanic effect, i.e., the formation of DC electric current flowing along the sample edges in response to AC electric field of the incident terahertz radiation, for two-dimensional Dirac materials including the systems with massive and massless charge carriers. The edge current direction is controlled by the AC field polarization. The spectral dependence of the current is determined by the carrier dispersion and the mechanism of carrier scattering, as shown for single-layer and bilayer graphene as examples.

**Keywords:** edge currents; high-frequency nonlinear transport; photogalvanic effect; two-dimensional Dirac structures; massive and massless fermions

## 1. Introduction

The discovery of graphene and other two-dimensional (2D) crystals opened a new page in the physics of low-dimensional systems [1,2] and triggered the research aimed at the development of efficient sources and detectors of terahertz radiation based on 2D Dirac materials [3,4]. In small-size samples, e.g., flakes obtained by mechanical exfoliation, the important and sometimes decisive role in the formation of photoelectric response is played by edges and nearby regions [5,6]. At the edges, the translational and space inversion symmetries are naturally broken, which gives rise to edge-related mechanisms of the photogalvanic effect [5–11] and the second harmonic generation [12–14].

The photocurrents flowing along the sample edges (the edge photogalvanic effect) were observed and studied in single-layer and bilayer graphene samples excited by terahertz radiation [5,6,10], also in an external magnetic field in the conditions of cyclotron resonance [9] and in the regime of the quantum Hall effect [15]. It is found that the edge photocurrent is induced by both linearly and circularly polarized radiation. Moreover, the photocurrent direction is controlled by the polarization of the incident radiation: the electric field direction with respect to the edge for the linearly polarized field and the photon helicity for the circularly polarized field. The edge photogalvanic effect in 2D structures can be considered as a low-dimensional analog of the surface photogalvanic effect studied in bulk semiconductor crystals and metal films and recently in nanocomposite films [16–22].

The microscopic theory of the edge photogalvanic effect in the spectral range of intraband transport has been developed so far for 2D systems with parabolic energy spectrum of charge carriers [6,8]. Here, we generalize the theory to the class of 2D Dirac materials. We present a comprehensive theoretical study of the edge currents for 2D systems with arbitrary dispersion  $\varepsilon(p)$  and arbitrary type of electron scattering in the 2D bulk. We show that the edge current is determined by the dispersion of carriers and the relaxation times of the first and second angular harmonics of the distribution function and compare the results for single-layer and bilayer graphene, which are examples of 2D systems with parabolic and linear energy spectra.



**Citation:** Durnev, M.V.; Tarasenko, S.A. Edge Currents Induced by AC Electric Field in Two-Dimensional Dirac Structures. *Appl. Sci.* **2023**, *13*, 4080. <https://doi.org/10.3390/app13074080>

Academic Editor: Gennady M. Mikheev

Received: 25 February 2023

Revised: 19 March 2023

Accepted: 20 March 2023

Published: 23 March 2023



**Copyright:** © 2023 by the authors. Licensee MDPI, Basel, Switzerland. This article is an open access article distributed under the terms and conditions of the Creative Commons Attribution (CC BY) license (<https://creativecommons.org/licenses/by/4.0/>).

## 2. Microscopic Theory

Consider an electromagnetic wave incident on the structure hosting a 2D electron gas occupying the  $(xy)$  half-plane at  $x \geq 0$ , see Figure 1. The AC electric field of the incident wave has the form  $E(t) = E \exp(-i\omega t) + c.c.$ , where  $E$  and  $\omega$  are the field amplitude and frequency, respectively, and the abbreviation “c.c.” denotes the complex conjugation. The AC electric field causes the back-and-forth in-plane motion of electrons. At the edge of the structure (here, at  $x = 0$ ), the AC motion of electrons gets distorted due to electron reflection from the edge and dynamic charge accumulation, which leads to an asymmetry of the high-frequency electron transport. This asymmetry results in the rectification of the AC current and, hence, the emergence of a DC current  $J_y$  flowing along the edge. As Figure 1 illustrates, the DC edge current can be excited by both linearly polarized and circularly polarized electromagnetic waves and the current direction is controlled by the wave polarization.

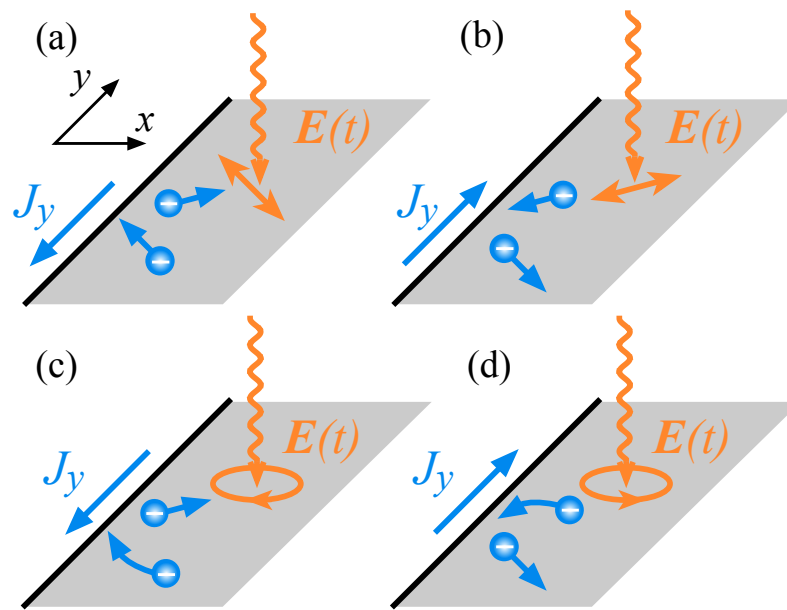


**Figure 1.** Illustration of the edge current formation. The back-and-forth motion of 2D carriers occupying the  $x \geq 0$  half-plane by linearly polarized (a,b) or circularly polarized (c,d) AC electric field results, due to electron scattering from the edge and dynamical charge accumulation, in the DC current  $J_y$  flowing along the edge. The edge current direction is controlled by the field polarization.

Now we present the microscopic theory of high-frequency non-linear electron transport and calculate the edge current. We consider the classical range of the electromagnetic wave frequencies, i.e.,  $\hbar\omega \ll E_F$ , where  $E_F$  is the Fermi energy of the 2D electron gas, and describe the electron kinetics by the Boltzmann equation

$$\frac{\partial f}{\partial t} + v_x \frac{\partial f}{\partial x} + e\mathcal{E}(x, t) \cdot \frac{\partial f}{\partial \mathbf{p}} = I\{f\}. \tag{1}$$

Here,  $f = f(\mathbf{p}, x, t)$  is the electron distribution function,  $\mathbf{p}$  and  $\varepsilon(p)$  are the electron momentum and energy, respectively,  $\mathbf{v} = d\varepsilon/d\mathbf{p} = v\mathbf{p}/p$  is the velocity,  $v = d\varepsilon/dp$ ,  $e$  is the electron charge,  $\mathcal{E}(x, t) = \mathcal{E}(x) \exp(-i\omega t) + c.c.$  is the local electric field acting upon the electrons, and  $I\{f\}$  is the collision integral. At this stage, we assume that the electron spectrum is isotropic in the 2D plane but do not specify the exact form of the dispersion  $\varepsilon(p)$ . The field  $\mathcal{E}(x)$  near the edge differs from the incident field  $E$  by the correction  $\delta E(x) \parallel x$  due to the screening produced by dynamical charge accumulation [6,23,24]. Therefore,  $\mathcal{E}_y = E_y$  whereas  $\mathcal{E}_x(x) \propto E_x$ .

At equilibrium, the electron distribution is isotropic and homogenous at  $x \geq 0$  and is described by the Fermi–Dirac function  $f_0(\epsilon)$ . In the presence of an AC electric field, the distribution function acquires corrections. We expand the resulting distribution function  $f(\mathbf{p}, x, t)$  in the series in the electric field amplitude as follows

$$f(\mathbf{p}, x, t) = f_0 + [f_1(\mathbf{p}, x) \exp(-i\omega t) + \text{c.c.}] + f_2(\mathbf{p}, x) + \dots, \tag{2}$$

where  $f_1$  is the first-order correction, which determines the linear (Drude) conductivity, and  $f_2$  is the time-independent second-order correction. The second-order correction oscillating at  $2\omega$  is not considered here since it does not contribute to DC electric current.

The density of DC electric current  $j_y(x)$  is determined by the asymmetric part of the correction  $f_2$  and is given by

$$j_y(x) = eg \sum_{\mathbf{p}} v_y f_2(\mathbf{p}, x), \tag{3}$$

where  $g$  is the factor that takes into account possible spin and valley degeneracy (e.g.,  $g = 2$  for GaAs quantum wells and  $g = 4$  for single-layer and bilayer graphene) and  $\sum_{\mathbf{p}} = (2\pi\hbar)^{-2} \int d^2\mathbf{p}$ .

Equation (1) with the perturbation term  $e\mathcal{E}(x, t) \cdot \partial f / \partial \mathbf{p}$  yields the following differential equations for  $f_1$  and  $f_2$

$$-i\omega f_1 + v_x \frac{\partial f_1}{\partial x} + e\mathcal{E}(x) \cdot \frac{\partial f_0}{\partial \mathbf{p}} = I\{f_1\}, \tag{4}$$

$$v_x \frac{\partial f_2}{\partial x} + \left[ e\mathcal{E}(x) \cdot \frac{\partial f_1^*}{\partial \mathbf{p}} + \text{c.c.} \right] = I\{f_2\}. \tag{5}$$

We solve Equations (4) and (5) in the approximation of elastic electron scattering in the bulk of the 2D system and for specular reflection of electrons from the edge. The latter implies that  $f(p_x, p_y, 0, t) = f(-p_x, p_y, 0, t)$  which also ensures the lack of electric current across the edge. Multiplying Equation (5) by the velocity  $v_y$  and averaging the resulting equation over the directions of  $\mathbf{p}$  one obtains

$$\left\langle v_x v_y \frac{\partial f_2}{\partial x} \right\rangle + \left\langle v_y \left( e\mathcal{E} \cdot \frac{\partial f_1^*}{\partial \mathbf{p}} + \text{c.c.} \right) \right\rangle = -\frac{\langle v_y f_2 \rangle}{\tau_1}, \tag{6}$$

where the angular brackets  $\langle \dots \rangle$  stand for the averaging and  $\tau_1$  is the momentum relaxation time (relaxation time of the first angular harmonic) defined as  $1/\tau_1 = -\langle \mathbf{v} I\{f\} \rangle / \langle \mathbf{v} f \rangle$ . Such a definition of  $\tau_1$  enables the consideration of its dependence on the electron energy  $\epsilon(p)$ . Equations (3) and (6) yield the equation for the current density

$$j_y(x) = -eg \sum_{\mathbf{p}} \tau_1 v_x v_y \frac{\partial f_2}{\partial x} - eg \sum_{\mathbf{p}} \tau_1 v_y \left( e\mathcal{E} \cdot \frac{\partial f_1^*}{\partial \mathbf{p}} + \text{c.c.} \right). \tag{7}$$

After the integration of the second term by parts, Equation (7) assumes the form

$$\begin{aligned} j_y(x) = & -eg \sum_{\mathbf{p}} \tau_1 v_x v_y \frac{\partial f_2}{\partial x} + e^2 g \sum_{\mathbf{p}} \left( \frac{\tau_1}{m} \right)' m v_x v_y (\mathcal{E}_x f_1^* + \text{c.c.}) \\ & + e^2 g \sum_{\mathbf{p}} \left[ \frac{\tau_1}{m} + \left( \frac{\tau_1}{m} \right)' \frac{mv^2}{2} - m \left( \frac{\tau_1}{m} \right)' \frac{v_x^2 - v_y^2}{2} \right] (E_y f_1^* + \text{c.c.}), \end{aligned} \tag{8}$$

where  $(\dots)' = d(\dots)/d\epsilon$  and  $m = p/v = p/(d\epsilon/dp)$  is the (energy-dependent) effective mass. In the case of parabolic dispersion  $\epsilon(p) = p^2/(2m^*)$  the effective mass  $m = m^*$  is energy-independent whereas for linear dispersion  $\epsilon(p) = v_0 p$  the effective mass  $m = \epsilon/v_0^2$  linearly depends on energy. Note that the mass  $m$  also determines the quasi-classical cyclotron motion. Equation (8) is valid for arbitrary dispersion and arbitrary boundary

conditions at the edge. Obviously, the DC current vanishes for the AC field polarized along or perpendicularly to the edge and emerges only if the incident field  $E$  has both  $x$  and  $y$  components. Therefore, the corrections  $f_1$  in the second and third terms on the right-hand side of Equation (8) should be calculated for the  $y$  and  $x$  components of the field, respectively.

For specular reflection of electrons from the edge, the second sum in Equation (8) vanishes since  $f_1$  in response to  $E_y$  is an even function of  $v_x$ . The third sum in Equation (8) can be rewritten via  $\partial f_1^*/\partial x$  using the equalities

$$i\omega \langle f_1 \rangle = \left\langle v_x \frac{\partial f_1}{\partial x} \right\rangle, \tag{9}$$

$$\left( i\omega - \frac{1}{\tau_2} \right) \left\langle \frac{v_x^2 - v_y^2}{2} f_1 \right\rangle = \left\langle v_x \frac{v_x^2 - v_y^2}{2} \frac{\partial f_1}{\partial x} \right\rangle, \tag{10}$$

which follow from Equation (4). Here,  $\tau_2$  is the relaxation time of the second angular harmonic of the distribution function defined as  $1/\tau_2 = -\langle (v_x^2 - v_y^2) I\{f\} \rangle / \langle (v_x^2 - v_y^2) f \rangle$ . Therefore, Equation (8) assumes the form

$$\begin{aligned} j_y(x) = & -eg \sum_p \tau_1 v_x v_y \frac{\partial f_2}{\partial x} + \frac{e^2 g}{\omega} \sum_p v_x \left[ \frac{\tau_1}{m} + \left( \frac{\tau_1}{m} \right)' \frac{mv^2}{2} \right] \left( iE_y \frac{\partial f_1^*}{\partial x} + \text{c.c} \right) \\ & + e^2 g \sum_p m v_x \frac{v_x^2 - v_y^2}{2} \left( \frac{\tau_1}{m} \right)' \left( \frac{\tau_2 E_y}{1 + i\omega\tau_2} \frac{\partial f_1^*}{\partial x} + \text{c.c} \right). \end{aligned} \tag{11}$$

The current density  $j_y(x)$  is determined by spatial derivatives of the distribution function and, as expected, vanishes in the 2D bulk where the electron distribution is homogenous.

The total electric current flowing along the edge is given by

$$J_y = \int_0^\infty j_y(x) dx. \tag{12}$$

Integrating Equation (11) over  $x$  we obtain

$$\begin{aligned} J_y = & -eg \sum_p \tau_1 v_x v_y [f_2(\mathbf{p}, \infty) - f_2(\mathbf{p}, 0)] \\ & + \left\{ i \frac{e^2 g}{\omega} \sum_p \left[ \frac{\tau_1}{m} + \left( \frac{\tau_1}{m} \right)' \frac{mv^2}{2} \right] v_x [f_1^*(\mathbf{p}, \infty) - f_1^*(\mathbf{p}, 0)] E_y + \text{c.c} \right\} \\ & + \left\{ e^2 g \sum_p \left( \frac{\tau_1}{m} \right)' \frac{m\tau_2}{1 + i\omega\tau_2} \frac{v_x^2 - v_y^2}{2} v_x [f_1^*(\mathbf{p}, \infty) - f_1^*(\mathbf{p}, 0)] E_y + \text{c.c} \right\}, \end{aligned} \tag{13}$$

where  $f_n(\mathbf{p}, 0)$  and  $f_n(\mathbf{p}, \infty)$  are the corrections to the distribution function at the edge and far from the edge, respectively. For the particular case of specular reflection of electrons from the edge, the functions  $f_1(\mathbf{p}, 0)$  and  $f_2(\mathbf{p}, 0)$  are even in  $p_x$  and, therefore, the sums with  $f_1(\mathbf{p}, 0)$  and  $f_2(\mathbf{p}, 0)$  vanish. As a result, the edge current  $J_y$  is determined by the functions  $f_1(\mathbf{p}, \infty)$  and  $f_2(\mathbf{p}, \infty)$  in the bulk where the actual field  $\mathcal{E}$  coincides with the incident field  $E$ . The sums with  $f_1(\mathbf{p}, \infty)$  and  $f_2(\mathbf{p}, \infty)$  can be readily calculated from Equations (4) and (5) neglecting spatial inhomogeneous terms and the electric field screening. Below, we do such calculations for the degenerate electron gas with the Fermi energy  $E_F$ .

The first-order correction in the 2D bulk has the form

$$f_1(\mathbf{p}, \infty) = -\frac{e\tau_1 f_0'}{1 - i\omega\tau_1} (\mathbf{v} \cdot \mathbf{E}). \tag{14}$$

Therefore, the second sum in Equation (13) is calculated as follows

$$ie g \sum_p \left[ \frac{\tau_1}{m} + \left( \frac{\tau_1}{m} \right)' \frac{mv^2}{2} \right] v_x f_1^*(\mathbf{p}, \infty) E_y + \text{c.c.} = \left[ \frac{\tau_1}{m} + \left( \frac{\tau_1}{m} \right)' \frac{mv^2}{2} \right]_{E_F} [i\sigma^*(\omega) E_x^* E_y + \text{c.c.}]$$

$$= \left[ \frac{\tau_1}{m} + \left( \frac{\tau_1}{m} \right)' \frac{mv^2}{2} \right]_{E_F} \text{Re} \sigma(\omega) (\omega \tau_1 S_2 - S_3), \quad (15)$$

where  $\sigma(\omega)$  is the conductivity,

$$\sigma(\omega) = -\frac{e^2 g}{2} \sum_p \frac{\tau_1 v^2 f_0'}{1 - i\omega \tau_1} = \frac{ne^2}{m} \frac{\tau_1}{1 - i\omega \tau_1}, \quad (16)$$

all the values are taken at the Fermi level,  $n = g \sum_p f_0$  is the carrier density, and  $S_2 = E_x E_y^* + E_x^* E_y$  and  $S_3 = i(E_x E_y^* - E_x^* E_y)$  are the Stokes parameters of the incident radiation. The third sum in Equation (13) is calculated as follows

$$e g \sum_p \left( \frac{\tau_1}{m} \right)' \frac{m \tau_2}{1 + i\omega \tau_2} \frac{v_x^2 - v_y^2}{2} v_x f_1^*(\mathbf{p}, \infty) E_y + \text{c.c.} = \frac{1}{4} \left( \frac{\tau_1}{m} \right)'_{E_F} \frac{mv^2 \tau_2 \sigma^*(\omega)}{1 + i\omega \tau_2} E_x^* E_y + \text{c.c.}$$

$$= \frac{1}{4} \left( \frac{\tau_1}{m} \right)'_{E_F} \frac{mv^2 \tau_2 \text{Re} \sigma(\omega)}{1 + (\omega \tau_2)^2} [(1 - \omega^2 \tau_1 \tau_2) S_2 + \omega(\tau_1 + \tau_2) S_3]. \quad (17)$$

Lastly, the sum with  $f_2(\mathbf{p}, \infty)$  in Equation (13) can be expressed with the help of Equation (5) via the sum with  $f_1(\mathbf{p}, \infty)$  as follows

$$\sum_p \tau_1 v_x v_y f_2(\mathbf{p}, \infty) = -e \sum_p \tau_1 \tau_2 v_x v_y \left( \mathbf{E} \cdot \frac{\partial f_1^*(\infty)}{\partial \mathbf{p}} + \text{c.c.} \right). \quad (18)$$

Integration of the right-hand side of Equation (18) by parts gives

$$\sum_p \tau_1 v_x v_y f_2(\mathbf{p}, \infty) = \left\{ e \sum_p \left[ \frac{\tau_1 \tau_2}{m} + \frac{m^2 v^2}{2} \left( \frac{\tau_1 \tau_2}{m^2} \right)' \right] (v_y E_x^* + v_x E_y^*) f_1(\mathbf{p}, \infty) + \text{c.c.} \right\}$$

$$+ \left\{ e \sum_p m^2 \left( \frac{\tau_1 \tau_2}{m^2} \right)' \frac{v_x^2 - v_y^2}{2} (v_y E_x^* - v_x E_y^*) f_1(\mathbf{p}, \infty) \right\}. \quad (19)$$

The above sums can be calculated similarly to the sums in Equations (15) and (17), which yields

$$g \sum_p \tau_1 v_x v_y f_2(\mathbf{p}, \infty) = 2 \left[ \frac{\tau_1 \tau_2}{m} + \frac{m^2 v^2}{4} \left( \frac{\tau_1 \tau_2}{m^2} \right)' \right]_{E_F} \text{Re} \sigma(\omega) S_2. \quad (20)$$

Finally, summing up all contributions to the edge current we obtain

$$J_y = \frac{e \text{Re} \sigma(\omega)}{m} \left\{ \tau_1 (\tau_1 - 2\tau_2) + \frac{m^2 v^2}{2} \left[ \frac{\tau_1}{2} \left( \frac{\tau_1}{m} \right)' - m \left( \frac{\tau_1 \tau_2}{m^2} \right)' \right] + \frac{m^2 v^2 (\tau_1 + \tau_2)}{4[1 + (\omega \tau_2)^2]} \left( \frac{\tau_1}{m} \right)' \right\} S_2$$

$$- \frac{e \text{Re} \sigma(\omega)}{m \omega} \left[ \tau_1 + \frac{m^2 v^2 [2 + \omega^2 \tau_2 (\tau_2 - \tau_1)]}{4[1 + (\omega \tau_2)^2]} \right] \left( \frac{\tau_1}{m} \right)' S_3. \quad (21)$$

Equation (21) represents the main result of this paper. It describes the DC edge current in 2D electron gas with an arbitrary electron dispersion  $\varepsilon(p)$  and arbitrary energy-dependent relaxation times.

For parabolic energy spectrum with  $\varepsilon(p) = p^2/(2m^*)$ , Equation (21) gives

$$\begin{aligned}
 J_y^{(\text{par})} &= \frac{e\text{Re}\sigma(\omega)}{m^*} \left\{ \tau_1(\tau_1 - 2\tau_2) + \left[ \frac{\tau_1\tau_1'}{2} - (\tau_1\tau_2)' \right] \varepsilon_F + \frac{(\tau_1 + \tau_2)\tau_1'\varepsilon_F}{2[1 + (\omega\tau_2)^2]} \right\} S_2 \\
 &- \frac{e\text{Re}\sigma(\omega)}{m^*\omega} \left\{ \tau_1 + \frac{2 + \omega^2\tau_2(\tau_2 - \tau_1)}{2(1 + \omega^2\tau_2^2)} \tau_1'\varepsilon_F \right\} S_3.
 \end{aligned}
 \tag{22}$$

This result was obtained previously in the approximation of a single energy-independent relaxation time ( $\tau_1 = \tau_2 = \text{const}$ ) in Ref. [6] and in the form of Equation (22) in Ref. [8].

For linear energy spectrum  $\varepsilon(p) = v_0p$ , Equation (21) gives

$$\begin{aligned}
 J_y^{(\text{lin})} &= \frac{ev_0^2\text{Re}\sigma(\omega)}{2\varepsilon_F} \left\{ \tau_1 \left( \frac{3\tau_1}{2} - 2\tau_2 \right) + \left[ \frac{\tau_1\tau_1'}{2} - (\tau_1\tau_2)' \right] \varepsilon_F + \frac{(\tau_1 + \tau_2)(\tau_1'\varepsilon_F - \tau_1)}{2[1 + (\omega\tau_2)^2]} \right\} S_2 \\
 &- \frac{ev_0^2\text{Re}\sigma(\omega)}{2\varepsilon_F\omega} \left\{ 2\tau_1 + \frac{[2 + \omega^2\tau_2(\tau_2 - \tau_1)](\tau_1'\varepsilon_F - \tau_1)}{2[1 + (\omega\tau_2)^2]} \right\} S_3.
 \end{aligned}
 \tag{23}$$

### 3. Results and Discussion

Now, we discuss the spectral and polarization dependence of the edge current in 2D systems with parabolic and linear dispersions, also for different scattering mechanisms. First, we note that the current  $J_y$  is proportional to the square of the electric field amplitude ( $S_2, S_3 \propto E^2$ ), i.e., to the intensity of the incident field. Therefore, it belongs to the class of photocurrents. Here, the photocurrent emerges due to the intraband (Drude-like) absorption of the electromagnetic field and is proportional to the real part of the high-frequency conductivity  $\sigma(\omega)$ .

The direction of the edge current (the polarity along the  $y$  axis) depends on the polarization state of the field via the Stokes parameters  $S_2 = (E_xE_y^* + E_yE_x^*)$  and  $S_3 = i(E_xE_y^* - E_yE_x^*)$ . The contribution  $J_y \propto S_2$  is induced by linearly polarized radiation. This current is maximal if the radiation is polarized at the angle  $\pm\pi/4$  with respect to the edge and vanishes if the radiation is polarized along or perpendicular to the edge, Figure 1a,b. The contribution  $J_y \propto S_3$  describes the edge current induced by circularly polarized radiation and its direction is controlled by the radiation helicity, Figure 1c,d.

Equation (21) is quite general and can be applied to a wide class of 2D systems, including conventional III-V and II-VI quantum wells, bilayer graphene, and transition metal dichalcogenide monolayers with the parabolic spectrum, graphene and HgTe/CdHgTe quantum wells of the critical thickness with the linear spectrum, and narrow-gap 2D systems with the Dirac-like spectrum  $\varepsilon(p) = v_0\sqrt{(m^*v_0)^2 + p^2}$ . Below, we calculate  $J_y$  for single-layer and bilayer graphene.

Figure 2 shows the frequency dependence of the edge photocurrent  $J_y$  in a 2D system with the linear dispersion law  $\varepsilon(p) = v_0p$ . The parameters used for calculations are given in the caption of Figure 2 and correspond to high-quality graphene [25] with the electron density  $n = 5 \times 10^{11} \text{ cm}^{-2}$ . The curves are calculated after Equation (23) for linearly polarized radiation with the electric field directed at the angle  $\pi/4$  with respect to the edge ( $S_2/E^2 = 1, S_3 = 0$ ) and for circularly polarized radiation ( $S_3/E^2 = 1, S_2 = 0$ ). We consider two model types of scattering potential: (i) short-range scatterers, resulting in the energy dependence of the relaxation times  $\tau_1 = 2\tau_2 \propto \varepsilon^{-1}$ , and (ii) charged scatterers with the Coulomb potential, resulting in  $\tau_1 = 3\tau_2 \propto \varepsilon$  [7]. For charged scatterers, the ratio  $\tau_{1,2}/m$  does not depend on energy and the edge current is given by  $J_y = e\text{Re}\sigma(\omega)v_0^2\tau_1^2(E_F)/3E_F$  for linearly polarized radiation and  $J_y = -e\text{Re}\sigma(\omega)v_0^2\tau_1(E_F)/\omega E_F$  for circularly polarized radiation. Hence, the frequency dependence of the edge currents excited by linearly and circularly polarized radiation are determined by  $\text{Re}\sigma(\omega) \propto 1/(1 + \omega^2\tau_1^2)$  and  $\text{Re}\sigma(\omega)/\omega$ , respectively. For short-range scatterers, all terms in Equation (21) contribute to the current, and the frequency dependence gets more complicated. In particular, the current induced by linearly polarized radiation is constant at low frequencies, changes its sign at an intermediate frequency, and decays as  $\propto \omega^{-2}$  at high frequencies. The circular contribution

for short-range scatterers behaves as  $\propto \omega$  at low frequencies, in contrast to the diverging behavior  $\propto \omega^{-1}$  for Coulomb scatterers. The current magnitude is  $J_y \sim 10$  nA for  $1 \text{ W/cm}^2$  of the radiation intensity.

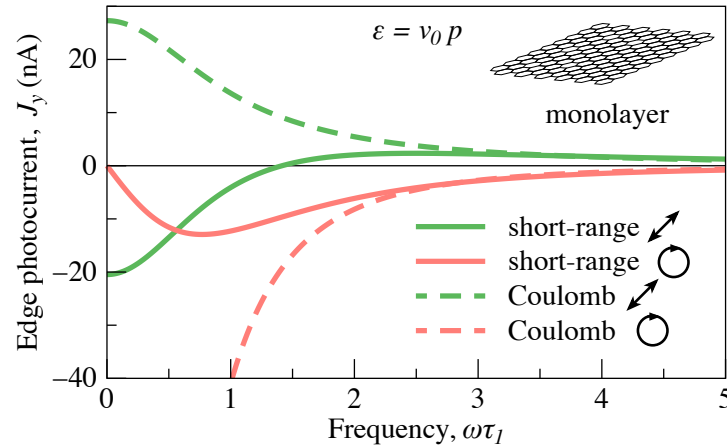


**Figure 2.** Frequency dependence of the edge current in 2D systems with a linear dispersion of carriers. Solid curves correspond to short-range scatterers and linearly polarized field with  $S_2 = E^2$  (green curve) and circularly polarized field with  $S_3 = E^2$  (red curve). Dashed curves present the results for scattering by charged impurities. The curves are calculated after Equation (23) for the parameters corresponding to single-layer graphene:  $v_0 = 10^8 \text{ cm/s}$ ,  $n = 5 \times 10^{11} \text{ cm}^{-2}$  (the Fermi energy  $E_F \approx 80 \text{ meV}$  and the effective mass at the Fermi level  $m \approx 0.013 m_0$ ),  $\tau_1(E_F) = 1 \text{ ps}$ , and  $E = 8 \text{ V/cm}$  corresponding to the radiation intensity  $I = 1 \text{ W/cm}^2$ .

Figure 3 shows the frequency dependence of the edge photocurrent  $J_y$  in the 2D system with the parabolic dispersion law  $\varepsilon(p) = p^2/2m^*$ . The parameters used for calculations are given in the caption of Figure 3 and correspond to high-quality bilayer graphene [6]. We use the same electron density  $n = 5 \times 10^{11} \text{ cm}^{-2}$  as in the case of single-layer graphene. The curves are calculated after Equation (22) for linearly polarized radiation with the electric field directed at the angle  $\pi/4$  with respect to the edge ( $S_2/E^2 = 1$ ,  $S_3 = 0$ ) and for circularly polarized radiation ( $S_3/E^2 = 1$ ,  $S_2 = 0$ ). For 2D systems with the parabolic spectrum and short-range scatterers, both the mass  $m$  and relaxation times  $\tau_1 = \tau_2$  are independent of energy and Equation (21) yields  $J_y = -e\text{Re}\sigma(\omega)\tau_1^2(E_F)/m^*$  for linearly polarized radiation and  $J_y = -e\text{Re}\sigma(\omega)\tau_1(E_F)/\omega m^*$  for circularly polarized radiation. For Coulomb scatterers,  $\tau_1 = 2\tau_2 \propto \varepsilon$ , and the frequency dependence of  $J_y$  is more complicated. Note that both the direction and magnitude of the current are determined to a great extent by the scattering mechanism. The calculated current magnitude for bilayer graphene is of the order of several nA for the radiation intensity  $1 \text{ W/cm}^2$  and is slightly smaller than that for monolayer graphene at the same electron density due to the larger effective mass in bilayer graphene.

Experimentally, edge photocurrents are detected as electric currents in short circuits or as voltage drops between contacts in open circuits [5,6,9,10]. If the sample is small and fully illuminated, the photocurrents are generated along all the edges and the resulting distribution of the photoinduced electric potential in the sample is determined by the edge photocurrents and the compensating drift currents in the sample. For linearly polarized radiation, the photocurrents generated along different edges are generally not equal because of different orientations of the edges with respect to the electric field polarization. For circularly polarized radiation, the edge photocurrents form a vortex whose winding direction depends on the radiation helicity. The photocurrents circulating around the sample produce, in turn, a magnetic field, which can be seen as a manifestation of the inverse Faraday effect.

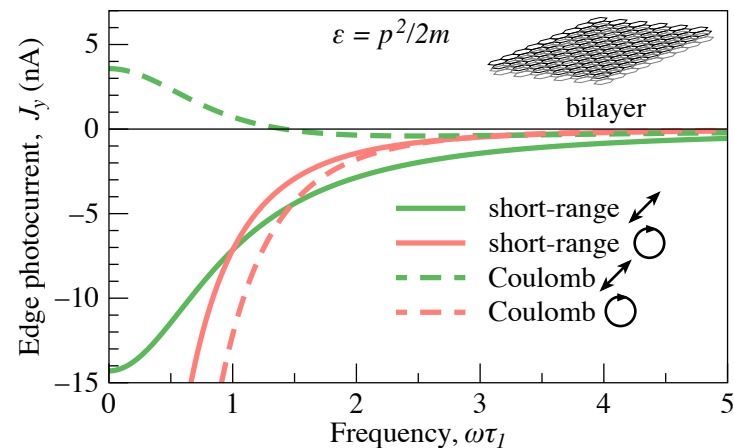


**Figure 3.** Frequency dependence of the edge photocurrent in 2D systems with parabolic energy dispersion. Solid curves correspond to short-range scatterers and linearly polarized field with  $S_2 = E^2$  (green curve) and circularly polarized field with  $S_3 = E^2$  (red curve). Dashed curves present the results for scattering by charged impurities. The curves are calculated after Equation (22) for parameters corresponding to bilayer graphene:  $m^* = 0.03 m_0$ ,  $n = 5 \times 10^{11} \text{ cm}^{-2}$ ,  $\tau_1(E_F) = 1 \text{ ps}$ , and  $E = 8 \text{ V/cm}$  corresponding to the radiation intensity  $I = 1 \text{ W/cm}^2$ .

#### 4. Conclusions

To conclude, we have developed a kinetic theory of the edge photogalvanic effect for the intraband electron transport in two-dimensional materials. It is shown that the back-and-forth motion of charge carriers by AC electric field of incident radiation is distorted at the edges of the sample resulting in direct electric currents flowing along the edges. The edge current direction is controlled by the radiation polarization while its spectral dependence is determined by the carrier dispersion and the mechanism of carrier scattering. We have obtained an analytical expression for the edge current valid for arbitrary dispersion law and scattering mechanism and analyzed the result for single-layer and bilayer graphene for electron scattering by short-range defects and Coulomb impurities. Considering the important role of edge regions in small-size samples such as flakes of two-dimensional crystals, one can expect that the edge photogalvanic effect will find applications in fast detectors of terahertz radiation and radiation polarization.

**Author Contributions:** M.V.D. and S.A.T. have contributed equality to the paper. All authors have read and agreed to the published version of the manuscript.

**Funding:** This research was supported by the Russian Science Foundation (project 21-72-00047).

**Institutional Review Board Statement:** Not applicable.

**Informed Consent Statement:** Not applicable.

**Data Availability Statement:** Not applicable.

**Conflicts of Interest:** The authors declare no conflict of interest.

#### Abbreviations

The following abbreviations are used in this manuscript:  
2D Two-dimensional

#### References

- Novoselov, K.S.; Jiang, D.; Schedin, F.; Booth, T.J.; Khotkevich, V.V.; Morozov, S.V.; Geim, A.K. Two-dimensional atomic crystals. *Proc. Natl. Acad. Sci. USA* **2005**, *102*, 10451. [[CrossRef](#)]
- Geim, A.K.; Grigorieva, I.V. Van der Waals heterostructures. *Nature* **2013**, *499*, 419. [[CrossRef](#)] [[PubMed](#)]

3. Koppens, F.H.L.; Mueller, T.; Avouris, P.; Ferrari, A.C.; Vitiello, M.S.; Polini, M. Photodetectors based on graphene, other two-dimensional materials and hybrid systems. *Nat. Nanotechnol.* **2014**, *9*, 780. [[CrossRef](#)] [[PubMed](#)]
4. Bandurin, D.A.; Svintsov, D.; Gayduchenko, I.; Xu, S.G.; Principi, A.; Moskotin, M.; Tretyakov, I.; Yagodkin, D.; Zhukov, S.; Taniguchi, T.; et al. Resonant terahertz detection using graphene plasmons. *Nat. Commun.* **2018**, *9*, 5392. [[CrossRef](#)]
5. Karch, J.; Drexler, C.; Olbrich, P.; Fehrenbacher, M.; Hirmer, M.; Glazov, M.M.; Tarasenko, S.A.; Ivchenko, E.L.; Birkner, B.; Eroms, J.; et al. Terahertz Radiation Driven Chiral Edge Currents in Graphene. *Phys. Rev. Lett.* **2011**, *107*, 276601. [[CrossRef](#)] [[PubMed](#)]
6. Candussio, S.; Durnev, M.V.; Tarasenko, S.A.; Yin, J.; Keil, J.; Yang, Y.; Son, S.K.; Mishchenko, A.; Plank, H.; Bel'kov, V.V.; et al. Edge photocurrent driven by terahertz electric field in bilayer graphene. *Phys. Rev. B* **2020**, *102*, 045406. [[CrossRef](#)]
7. Glazov, M.; Ganichev, S. High frequency electric field induced nonlinear effects in graphene. *Phys. Rep.* **2014**, *535*, 101. [[CrossRef](#)]
8. Durnev, M.V.; Tarasenko, S.A. Rectification of AC Electric Current at the Edge of 2D Electron Gas. *Phys. Status Solidi (B)* **2021**, *258*, 2000291. [[CrossRef](#)]
9. Candussio, S.; Durnev, M.V.; Slizovskiy, S.; Jötten, T.; Keil, J.; Bel'kov, V.V.; Yin, J.; Yang, Y.; Son, S.K.; Mishchenko, A.; et al. Edge photocurrent in bilayer graphene due to inter-Landau-level transitions. *Phys. Rev. B* **2021**, *103*, 125408. [[CrossRef](#)]
10. Candussio, S.; Golub, L.E.; Bernreuter, S.; Jötten, T.; Rockinger, T.; Watanabe, K.; Taniguchi, T.; Eroms, J.; Weiss, D.; Ganichev, S.D. Nonlinear intensity dependence of edge photocurrents in graphene induced by terahertz radiation. *Phys. Rev. B* **2021**, *104*, 155404. [[CrossRef](#)]
11. Durnev, M.V.; Tarasenko, S.A. Edge photogalvanic effect caused by optical alignment of carrier momenta in two-dimensional Dirac materials. *Phys. Rev. B* **2021**, *103*, 165411. [[CrossRef](#)]
12. Yin, X.; Ye, Z.; Chenet, D.A.; Ye, Y.; O'Brien, K.; Hone, J.C.; Zhang, X. Edge Nonlinear Optics on a MoS<sub>2</sub> Atomic Monolayer. *Science* **2014**, *344*, 488. [[CrossRef](#)] [[PubMed](#)]
13. Mishina, E.D.; Sherstyuk, N.E.; Shestakova, A.P.; Lavrov, S.D.; Semin, S.V.; Sigov, A.S.; Mitioglu, A.; Anghel, S.; Kulyuk, L. Edge effects in second-harmonic generation in nanoscale layers of transition-metal dichalcogenides. *Semiconductors* **2015**, *49*, 791. [[CrossRef](#)]
14. Durnev, M.V.; Tarasenko, S.A. Second harmonic generation at the edge of a two-dimensional electron gas. *Phys. Rev. B* **2022**, *106*, 125426. [[CrossRef](#)]
15. Plank, H.; Durnev, M.V.; Candussio, S.; Pernul, J.; Dantscher, K.M.; Mönch, E.; Sandner, A.; Eroms, J.; Weiss, D.; Bel'kov, V.V.; et al. Edge currents driven by terahertz radiation in graphene in quantum Hall regime. *2D Mater.* **2019**, *6*, 011002. [[CrossRef](#)]
16. Magarill, L.I.; Entin, M.V. Photogalvanic effect in films. *Sov. Phys. Solid State* **1979**, *21*, 743.
17. Alperovich, V.L.; Belinicher, V.I.; Novikov, V.N.; Terekhov, A.S. Surface photovoltaic effect in solids. Theory and experiment for interband transitions in gallium arsenide. *Sov. Phys. JETP* **1981**, *53*, 1201.
18. Alperovich, V.L.; Minaev, A.O.; Terekhov, A.S. Ballistic electron transport through epitaxial GaAs films in a magnetically induced surface photocurrent. *JETP Lett.* **1989**, *49*, 702.
19. Gurevich, V.L.; Laiho, R. Photomagnetism of metals: Microscopic theory of the photoinduced surface current. *Phys. Rev. B* **1993**, *48*, 8307–8316. [[CrossRef](#)]
20. Schmidt, C.B.; Priyadarshi, S.; Tarasenko, S.A.; Bieler, M. Ultrafast magneto-photocurrents in GaAs: Separation of surface and bulk contributions. *Appl. Phys. Lett.* **2015**, *106*, 142108. [[CrossRef](#)]
21. Mikheev, G.M.; Saushin, A.S.; Styapshin, V.M.; Svirko, Y.P. Interplay of the photon drag and the surface photogalvanic effects in the metal-semiconductor nanocomposite. *Sci. Rep.* **2018**, *8*, 8644. [[CrossRef](#)] [[PubMed](#)]
22. Mikheev, G.M.; Fateev, A.E.; Kogai, V.Y.; Mogileva, T.N.; Vanyukov, V.V.; Svirko, Y.P. Helicity dependent temporal profile of the semiconductor thin film photoresponse. *Appl. Phys. Lett.* **2021**, *118*, 201105. [[CrossRef](#)]
23. Volkov, V.; Mikhailov, S. Edge magnetoplasmons: Low frequency weakly damped excitations in inhomogeneous two-dimensional electron system. *JETP* **1988**, *67*, 1639.
24. Zabolotnykh, A.A.; Volkov, V.A. Interaction of gated and ungated plasmons in two-dimensional electron systems. *Phys. Rev. B* **2019**, *99*, 165304. [[CrossRef](#)]
25. Castro Neto, A.H.; Guinea, F.; Peres, N.M.R.; Novoselov, K.S.; Geim, A.K. The electronic properties of graphene. *Rev. Mod. Phys.* **2009**, *81*, 109. [[CrossRef](#)]

**Disclaimer/Publisher's Note:** The statements, opinions and data contained in all publications are solely those of the individual author(s) and contributor(s) and not of MDPI and/or the editor(s). MDPI and/or the editor(s) disclaim responsibility for any injury to people or property resulting from any ideas, methods, instructions or products referred to in the content.